

Estimation of effluent nutrients in municipal MBBR process

Tiina M. Komulainen^{a,*} Abdul Malik Baqeri^a Einar Neramo^a Arvind Keprate^a Torgeir Saltnes^b Katrine Marsten Jansen^c Olga Korostynska^a

^aOslo Metropolitan University, Norway, ^bHias How2O, Norway, ^cHias IKS, Norway
*tiina.komulainen@oslomet.no

Abstract

The recently updated European Union's Urban Waste Water Treatment Directive proposal, European Green Deal, Biodiversity Strategy for 2030, and EU's Energy System Integration highlight a pressing need for innovative biological nutrient removal processes and energy-efficient control methods to reduce pollution and minimize the carbon footprint at water resource recovery facilities. The aim of the PACBAL research project is to develop estimation methods for nutrient profile in a novel industrial Moving Bed Biofilm Reactor (MBBR) process. This study devises and assesses a range of data-driven methods to estimate effluent phosphorus concentration by utilizing a combination of real sensors with software models. The resulting virtual sensor could facilitate the design of energy-efficient control strategies. The case study data are collected from the MBBR process at Hias water resource recovery facility in Norway. Data sets from December 2022 to March 2023 include varying weather conditions, such as rain, dry, and snow. The Hias Process consists of three anaerobic and seven aerobic zones, where biomass carriers removes over 90 percent of the phosphorus from the wastewater in simultaneous biological processes. The industrial online measurements include wastewater flowrate, aeration rates, dissolved oxygen and nutrients COD and NO_2^-/NO_3^- at inlet and total suspended solids at outlet. Dynamic data-driven models including transfer functions, state-space models and ARX models, were developed and compared to estimate the outlet phosphorus concentration. Model fitness to validation data was around 7% with ARX models, and up to 18% with transfer function models and state-space models. The first and second order models gave similar results. The state-space models will be developed further and implemented to into virtual sensors that will enable energy-efficient control strategy development.

1 Introduction

There is a significant demand for novel biological nutrient removal processes and energy-effective control methods for minimization of carbon footprint and environmental pollution at wastewater resource recovery facilities (WRRF). As the European Commission has proposed an updated urban waste water treatment directive (European Commission, 2022), stricter requirements will be set for the removal of nutrients such as phosphorus, carbon and nitrogen. Water resource recovery facilities use approximately one percent of the total energy consumption in the European union. EU plan on energy system integration (European Commission, 2021) requires actions on energy efficiency that are necessary to convert the WRRFs from an energy consumer to energy-neutral user, or even an energy producer. At the municipal WRRF the primary wastewater treatment, clarification, is followed by a secondary treatment process, which removes nutrients such as phosphorus, carbon and nitrogen. The secondary treatment process relies either on chemical additions or biological process. Hias How2O has developed a novel continuous-flow moving bed biofilm reactor process with enhanced biological phosphorus re-

moval (MBBR-EBPR) and simultaneous nitrification and denitrification as described in Rudi et al. (2019). This process is an alternative to the biological process with an activated sludge. In the Hias Process, large amounts of small biofilm carriers, submerged in the wastewater, circulate through the ten process stages while the nutrients are removed from the wastewater in simultaneous biological processes in different layers of the biofilm. Soluble phosphorus (PO_4) in wastewater is removed biologically by phosphorus accumulating organisms (PAO) that grow on biofilm carriers.

The first step towards energy-effective control is development of dynamic models between the Hias Process inputs and effluent nutrient composition. Hence, we need to develop a dynamic model that can reproduce effluent nutrient composition accurately enough based on the Hias process inputs.

Moving bed bioreactor process can be modeled with ASM2D model as described by Henze et al. (1999). Application of the ASM2D model for the Hias Process with ten stages, would require estimation of 430 parameters and simultaneous solution of 210 rate equations. Hence, ASM2D model in its original form is too complicated with the current instrumentation.

Nair et al. (2019) have simplified the ASM2D model to include 8 components and 7 process rate equations, 2 stoichiometric constants, 11 saturation coefficients and 7 rate constants for both anaerobic and aerobic stages. Therefore, the ASM2D model, as it currently stands, is overly complex given the available instrumentation. The ASM2D model is further simplified for anaerobic basins with 3 components and 3 rate equations in Nair et al. (2020). Nair et al have demonstrated soft-sensor concept with Kalman filter for laboratory pilot system with one tank. Due to the available instrumentation in the Hias Process, this approach cannot be tested either.

Data-driven methods do not require a specific set of instrumentation, and several recent papers have reported successful applications to effluent prediction using multivariate linear regression (Tomperi & Leiviskä, 2018), feedforward-backpropagation networks (El-Rawy et al., 2021), and time-series models and machine learning models (Ly et al., 2022). In a recent master thesis (Nermo, 2023) transfer function models were developed to predict the Hias Process effluent phosphorus. In this article we continue Nermo's work by refining the input variable set and developing time-series models and state-space models.

1.1 Aim and research questions

The main obstacles for development of novel energy and emission efficient control strategies are the scarcity and cost of online measurements of nutrients in municipal WRRFs. Control strategy development requires models that sufficiently reproduce the nutrient dynamics of the plant based on available measurements. Hence, the aim of this work is to develop and compare different data-driven modeling approaches that enable control strategy development. Research question: Which data-driven models are most effective in predicting nutrient variations in the Hias Process effluent?

2 Materials and methods

2.1 Software

Matlab software package version R2023a was used for the simulations and System Identification Toolbox for modeling. The simulation method was ode23s with automatic settings for the time step and error tolerance.

2.2 The Hias Process and instrumentation

The Hias Process with instrumentation is illustrated in Figure 1. The clarified influent and the recirculated biofilm carriers on a conveyor belt enter the anaerobic basins. The water and biofilm carriers float through the process with gravity. The three anaerobic basins

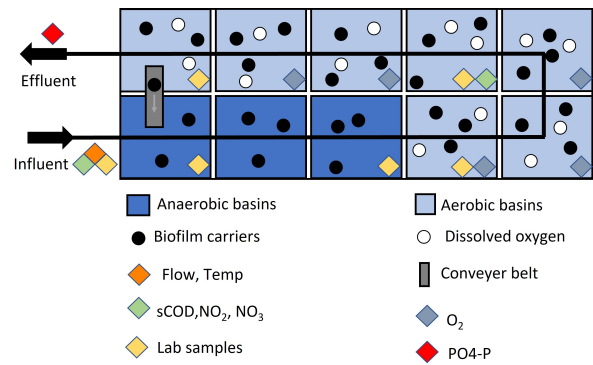


Figure 1. The Hias Process with instrumentation

are mixed to ensure sufficient distribution of biofilm carriers in the water. Aeration in the following seven basins ensures sufficient dissolved oxygen concentrations for aerobic nutrient removal. The Hias Process instrumentation includes continuous measurements of flowrates and nutrients compositions. Influent COD , NO_2 and NO_3 are measured continuously with the spectrophotometric instrument. Effluent phosphorus is measured using an online-analyzer with 10 minutes sampling time. These measurement as listed in Table 1.

Table 1. Online measurements

Symbol	Description	Unit
F	Water flowrate inlet	m^3/h
T	Temperature inlet	$^{\circ}C$
COD	COD inlet, basin7	g/m^3
NOX	$NO_2 + NO_3$ inlet, basin7	g/m^3
FO_i	Aeration rate basin 4-10	m^3/h
DO_i	Oxygen basin 4-10	m^3/h
TSS_{out}	Total suspended solids out Hias Process	g/m^3
TSS_{disc}	Total suspended solids after disc filter	g/m^3
PO_{4out}	PO_4 effluent	g/m^3

2.3 Data collection and pre-processing

The Industrial IoT platform KYB, developed by Digiread Connect, was used for uploading and standardizing operational data. The online data sets and laboratory data sets were collected in .csv format. The outliers in the online data set were first removed. Then, the missing values in the online data sets were filled. The correlations between variables were studied with a heatmap.

2.4 Data-driven dynamic models

The data-driven models suitable for control strategy design are desirable for the project, hence transfer function models, state-space models and time-series models were chosen. These linear models can be developed by following the system identification procedure by (Ljung, 1999). First, the data sets for modeling and validation are chosen. Then, a set of input and output variables is composed, and time delays are calculated between each input variables and output variable. The data is imported to the Matlab System Identification toolbox and model type is chosen. Lower order models are preferable to avoid modeling of noise. The identified models are compared using the fitness index and mean square error.

A first order transfer function model between inputs $U_i(s)$ and output $Y(s)$ consist of gain (K_p), delay (T_d), and time constant (T_{p1}) is presented in Equation 1:

$$TF(s) = \frac{Y(s)}{U_i(s)} = \frac{K_p}{(T_{p1}s + 1)} e^{-T_d s} \quad (1)$$

The time series model, an auto-regressive model with exogenous inputs (ARX) are presented in the equation 2. The model output $y(t)$ has order of 2, and the model inputs $u(t)$ have order of 2 with time delay td .

$$\begin{aligned} y(t) - a_1 y(t-1) - a_2 y(t-2) \\ = b_{i1} u(t-td) + b_{i2} u(t-td-1) + e(t) \end{aligned} \quad (2)$$

A state-space model is presented in equation 3. The derivative of the state $x(t)$ is related to the model inputs $u(t)$ with delays td via coefficient matrices A and B, and to the model error $e(t)$ with coefficient K. The measurement $y(t)$ is related to the state $x(t)$ via matrix C. The error $e(t)$ is calculated as difference between the model prediction and the real measurement. The measurement $y(t)$ is not affected by inputs $u(t)$ and hence, D matrix is zero.

$$\begin{aligned} \frac{dx(t)}{dt} &= Ax(t) + Bu(t-td) + Ke(t) \\ y(t) &= Cx(t) + Du(t-td) + e(t) \end{aligned} \quad (3)$$

The data-driven models are compared with each other using the fitness index (FIT) between the real measurements $y_{i,meas}$, the mean values of the real measurements $y_{i,mean}$, and the model calculated output $y_{i,model}$ in Equation 4, where norm is the Euclidean norm.

$$FIT = \left(1 - \frac{\text{norm}(y_{i,meas} - y_{i,model})}{\text{norm}(y_{i,meas} - y_{i,mean})}\right) 100 \quad (4)$$

Table 2. Pre-processing of input and output variables

Variable	Scaling	Scaled mean	Scaled stdev
F	3.6/1000	0.3184	0.0777
COD	/1000	0.4602	0.1015
NOX	/10	0.3566	0.1548
$FO5$	/1000	1.7614	0.7151
$FO8$	/1000	0.7833	0.2815
ΔTSS	/1000	0.1552	0.0323
PO_{4out}	no scaling	0.2236	0.1024

3 Results

3.1 Data collection and selection of test data

The data was screened and quality of measurements were assessed. Due to many missing measurements, inlet temperature, COD and NOX in basin 7 were omitted from the data set. The estimation period was 1.12.2022-31.1.2023 and the validation period was 1.2.2023-31.3.2023.

3.2 Data pre-processing

The outliers in the data set were identified based on the three standard deviation rule, and removed. Then, the missing values in the data sets were filled in using Matlab knnimp function based on nearest-neighbor imputation method. The data was analyzed with pair plot (not included here), which shows that the data is highly nonlinear, and thus z-normalization cannot be applied. The data were scaled by scalar multiplication as given in Table 2 and the means (Table 2) were removed.

3.3 Output variable

The only available output variable in the data sets is effluent phosphorus concentration PO_{4out} .

3.4 Input variable selection

The measured input variables include: inlet wastewater flowrate F , inlet carbon COD , inlet nitrate and nitrite NOX , aeration rates $FO_4 \dots FO_{10}$. The dissolved oxygen concentration in aerobic basins $DO_4 \dots DO_9$ are dependent on aeration rate. Results of Nermo's Master's Thesis (Nermo, 2023) pointed into careful selection of input variables, and creation of extra variable representing the biomass storage capacity. The biomass carrier's storage capacity is based on phosphorus removal during previous biomass carrier cycle around the ten basins. The storage capacity was modeled with the difference of total suspended solids between treated water out of the Hias Process TSS_{out} and

the total suspended solids after the disc filter TSS_{disc} , as in Equation 5:

$$\Delta TSS(t) = TSS_{out}(t) - TSS_{disc}(t) \quad (5)$$

A heat map of correlations between the variables was plotted in Figure 2.

The heat map shows that aeration rates in basins 4 - 10 ($FO_4 \dots FO_{10}$) are highly correlated with each other and PO_{4out} . Hence, we selected two aeration rates, FO_5 and FO_8 for input variables representing the manipulated variables of the system. Dissolved oxygen measurements are not included as these are state variables and highly correlated with the aeration rates. Inlet wastewater flow rate (F), inlet carbon (COD), inlet nitrite and nitrate concentration (NOX) and total suspended solids (ΔTSS) are the measured disturbance variables of the system. The biological mechanism of (COD) is improving phosphorus removal whereas (NOX) would hinder phosphorus removal. It is surprising that both are correlated positively with PO_{4out} , hence both are included as input variables. Storage capacity (ΔTSS) is mildly correlated with PO_{4out} , and included as input variable. The inlet flowrate (F) should have an effect on the PO_{4out} , but the correlation is low. However, (F) is included as input variable. Based on the biological phosphorus removal process (MBBR-EBPR), we could expect that increased flowrate would dilute PO_{4out} (- sign), NOX to hinder removal and increase the PO_{4out} (+ sign), aeration rates (FO_i) to improve the removal and decrease the PO_{4out} (- sign), and storage capacity ΔTSS to improve the removal and decrease the PO_{4out} (- sign). Based on laboratory measurements, inlet COD is very correlated with inlet phosphorus PO_{4in} , and increase in COD means increase in PO_{4in} , which in turn increases PO_{4out} (+sign). However, the heat map in Figure 2 gives positive correlations between PO_{4out} and the selected inputs.

3.5 Input delays and sampling time

The Hias process has significant time delays between the process inlet and outlet. The delay can be calculated as volume of ten basins divided by average wastewater flowrate $F_{average}$ as in Equation 6. The time delay is time variant, but in this work estimated as time invariant.

$$Td = \frac{V_{total}}{F_{average}} = \frac{10 \cdot 215m^3}{5.58m^3/min} = 385min \quad (6)$$

The six input variables consists of inlet water flowrate F , the inlet carbon composition COD , inlet nitrate and nitrite composition NOX and total suspended solids ΔTSS all four with a delay of 385min, aeration rate in basin 5 FO_5 with delay of 270 min, and aeration rate in basin 8 FO_8 with delay of 115 min. The data was

imported to Matlab system identification toolbox with sampling time of 10 minutes.

3.6 Transfer functions

The estimated transfer function model parameters and error indices for estimation and validation data sets are given in Table 3 for TF0, a pure gain with a delay, and Table 4 for TF1, a first order model with delay. Time constants and delay are given in minutes. The signs of the gains K_p in the TF0 model are not quite as expected, but the modeling results are acceptable for estimation data (7%) and validation data (18%) and the model follows dynamic trends. The first order transfer function model follows the dynamic trends in the data as illustrated in Figure 3. The time constants T_p of the second order model TF1 4 are unacceptable large and give no physical interpretation, however the results for estimation and validation data are acceptable. We choose further to use the first order transfer function model TF0.

3.7 Time-series models

Time-series models in the format of auto-regressive with exogenous inputs were developed and tested. The input and output variables, and input delays were the same as for the transfer functions. The parameters and fitness index are shown in Table 5 for first order ARX110 model and in Table 6 for second order ARX220 model. The signs of the coefficients b_{i1} in the ARX110 model are not quite as expected, as coefficients for the aeration rates FO_i are positive. However the modeling results are very good for estimation data (69%) and acceptable for validation data (7%) and the model follows most of the dynamic trends in Figure 4. The results for the second order ARX model are similar to the first order model (70% and 7%), hence we work further with the first order model.

3.8 State-space models

State-space models were developed and tested. The input and output variables, and input delays, were the same as for the transfer functions. A first order (SS1) and a second order (SS2) state space model were identified. The parameters and results are shown in Table 7 for the SS1. The results for the second order state-space model were not successful. The signs of the coefficients b_{i1} in the SS1 model are logical for the phosphorus removal phenomena, except for aeration rates FO_5 and FO_8 . Coefficient A for previous phosphorus measurements is ten fold compared to the input coefficients B, which implicates that the model is relies heavily on the previous effluent phosphorus measurements. As the data set is rather large, the parameter uncertainties for A, B and C are also very large. However, the modeling results are sufficient for estimation

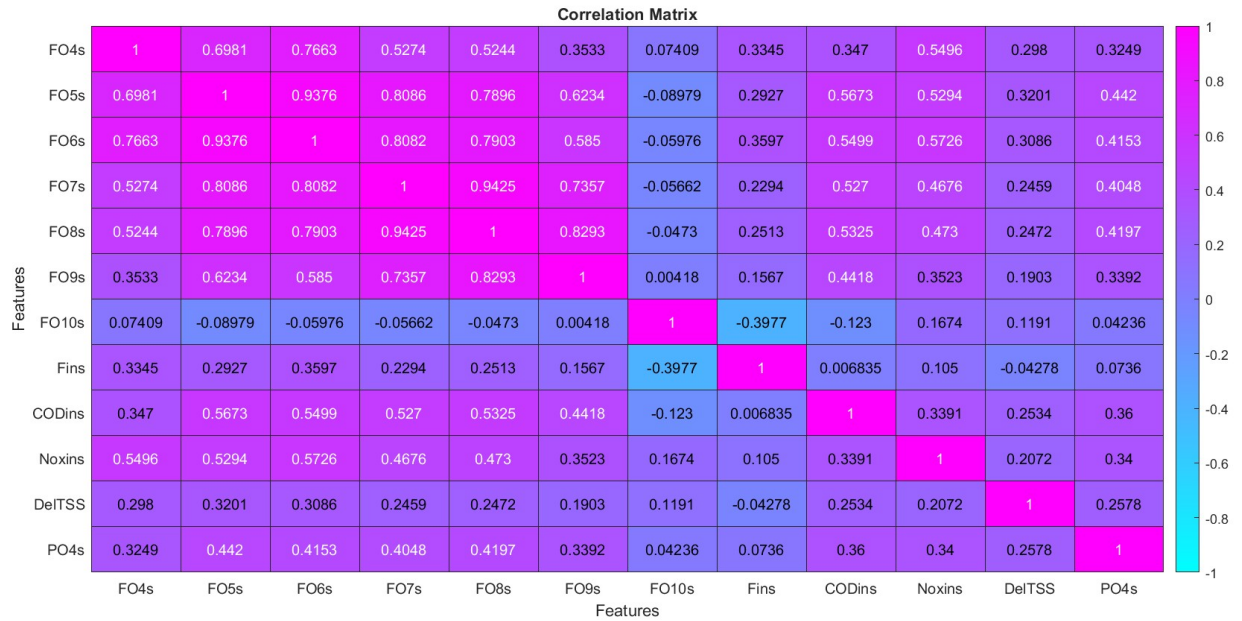


Figure 2. Heatmap between variables

data (6%) and good for validation data (18%) and the model follows dynamic trends in Figure 5. Hence, we work further with the first order state-space model.

Table 3. TF0 parameters

Input	Td	Kp
F	385	$-6.68 \cdot 10^{-2}$
COD	385	$0.9857 \cdot 10^{-2}$
NOX	385	$8.989 \cdot 10^{-2}$
FO5	270	$2.317 \cdot 10^{-2}$
FO8	115	$7.627 \cdot 10^{-2}$
ΔTSS	385	$23.24 \cdot 10^{-2}$
FITest	6.518	
FITval	17.67	

Table 4. TF1 parameters

Input	Td	Kp	Tp
F	385	0.293	327.5
COD	385	2.5	24838
NOX	385	0.24	159611
FO5	270	1.27	$6.21e-7$
FO8	115	2.6	20177
ΔTSS	385	-11.3	27322
FITest	15.89		
FITval	10.46		

Table 5. ARX110 parameters

Output	constant	a_1
$PO_{4,out}$	1	0.9497
Input	delay	b_{i1}
F	385	$6.067 \cdot 10^{-3}$
COD	385	$4.392 \cdot 10^{-3}$
NOX	385	$0.6784 \cdot 10^{-3}$
FO5	270	$0.3634 \cdot 10^{-3}$
FO8	115	$4.21 \cdot 10^{-3}$
ΔTSS	385	$-3.26 \cdot 10^{-3}$
FITest	68.85	
FITval	6.743	

Table 6. ARX220 parameters

Output	constant	a_1	a_2
$PO_{4,out}$	1	0.6529	0.3123
Input	delay	b_{i1}	b_{i2}
F	385	$11.09 \cdot 10^{-3}$	$-3.206 \cdot 10^{-3}$
COD	385	$6.826 \cdot 10^{-3}$	$-3.953 \cdot 10^{-3}$
NOX	385	$-2.044 \cdot 10^{-3}$	$+1.693 \cdot 10^{-3}$
FO5	270	$0.7614 \cdot 10^{-3}$	$-0.7147 \cdot 10^{-3}$
FO8	115	$0.7298 \cdot 10^{-3}$	$+3.233 \cdot 10^{-3}$
ΔTSS	385	$-37.75 \cdot 10^{-3}$	$+43.62 \cdot 10^{-3}$
FITest	70.42		
FITval	6.5		

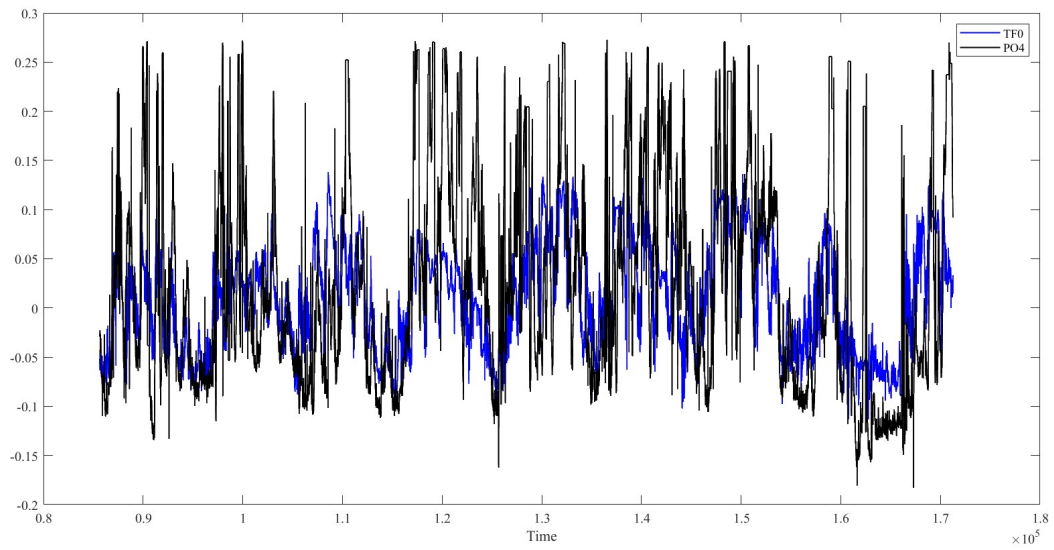


Figure 3. Scaled $PO_{4,out}$ measurement with black and TF0 estimate with blue, time in minutes.

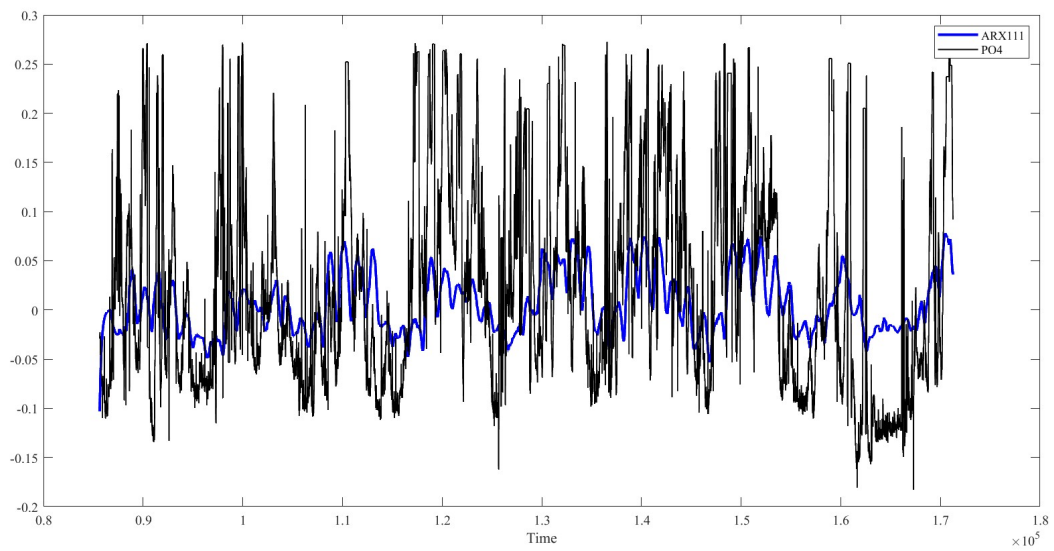


Figure 4. Scaled $PO_{4,out}$ measurement with black and ARX110 estimate with blue, time in minutes.

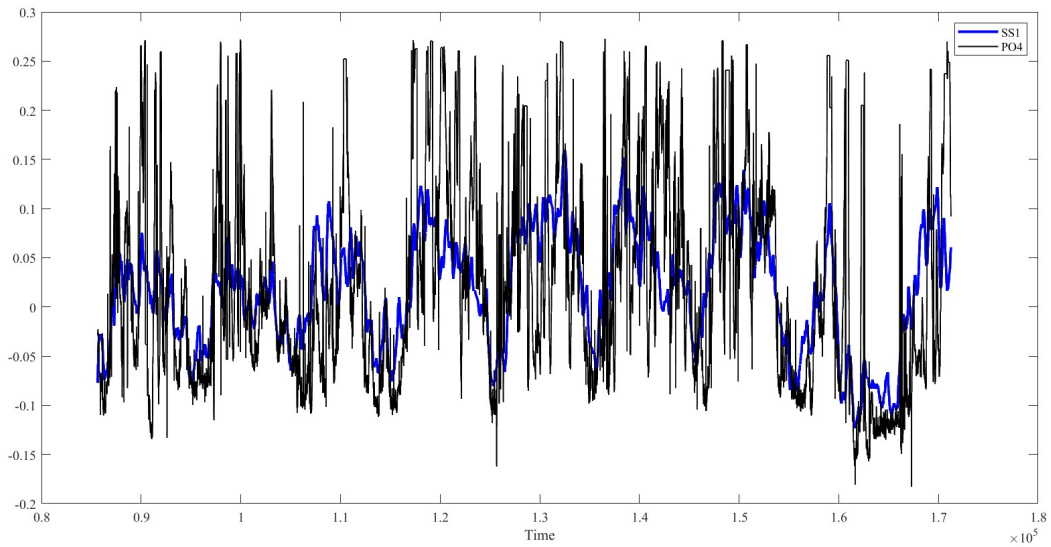


Figure 5. Scaled $PO_{4,out}$ measurement with black and SS1 estimate with blue, time in minutes.

Table 7. SS1 parameters

State	-	a_1
$x(t)$	-	$-72.92 \cdot 10^{-4}$
Inputs	delay	b_{i1}
F	385	$-3.731 \cdot 10^{-4}$
COD	385	$0.256 \cdot 10^{-4}$
NOX	385	$1.548 \cdot 10^{-4}$
FO5	270	$0.139 \cdot 10^{-4}$
FO8	115	$0.973 \cdot 10^{-4}$
ΔTSS	385	$-1.624 \cdot 10^{-4}$
Output	-	c_1
$PO_{4,out}$	-	7.578
FITest	6.178	
FITval	18.3	

4 Discussion and summary

Three data-driven modeling methods were tested for the four months data set from Hias municipal water resource recycling facility. Selection of input variables and determination of the input delays had most effect on the modeling accuracy. Using all the aeration rates and inlet flowrate, COD and NOX with the fitness index was around 1 % and the model was vaguely following the dynamics in the data (Nermo, 2023). Introducing the storage capacity estimated with difference of total suspended solids ΔTSS and reducing number of input variables (aeration rates FO_i) and fixing the input delay increased the fitness index significantly. We tried to reduce the number of inputs further by omitting the other aeration rate FO_8 , but this did not improve the results.

The model fitness to estimation data was best with time-series models, around 70%. The model fitness to validation data was best with state-space models, 18%. All the first order models follow the dynamic changes in the data. The model parameter signs did not have quite the logical interpretation to the biological phosphorus removal phenomena between the input and output variables. As the data set is rather large, the parameter uncertainty is large, and an estimation method updating the model output, such as Kalman filter, could be developed for the online application. The answer to our research question is: state-space model can reproduce nutrient variations in the Hias Process with sufficient accuracy. Hence, we work further with the first order state space model and prepare an online application estimating the effluent nutrient concentration.

Further work

Further work will encompass work on data pre-processing methods suitable for online use. We will test different input variables sets, possibly excluding FO_8 and including dissolved oxygen DO_5 as state variable for state-space model. With this model we will develop and test novel control strategies for the Hias Process.

Further work is suggested on developing sub-models for the Hias Process that estimate phosphorus $PO_{4,out}$ concentration in basins with newly installed conductivity and redox-potential measurements. Potentially these virtual measurements of phosphorus in the process can then be used as inputs for the outlet phosphorus modeling.

5 Acknowledgements and contributions

RFF Innlandet, Norway, is gratefully acknowledged for funding the PACBAL project (nr 337727).

Fruitful discussions with Oulu University researchers Jani Tomperi, Henri Pörhö and Esko Juuso, and CEIWA research project, are gratefully acknowledged for inspiration on model types and input variable selection.

Torgeir Saltnes at Hias How2O, Katrine Marsten Jansen from Hias IKS water resource recycling facility and provided valuable insights in the Hias Process. Tobias Kortén (Hias IKS) and Katrine Marsten Jansen have supported data collection. Axel Tveiten Bech and Ola Solli Grønningsæter from Digitread Connect have implemented IoT platform and performed online data collection. Anders Øfsti (Hias How2O) and Katrine Marsten Jansen (Hias IKS) have reviewed the article.

Professor Tiina Komulainen is the principal investigator of the project. She has supervised modeling work, provided the initial idea on input-output design and data-driven model types and structures. She has also prepared the article draft. Master student Einar Nermo done initial work on identifying transfer functions. Research assistant A. Malik Baqeri has continued the system identification work, improved the data preprocessing methods and identified the data-driven models under Professor Komulainen's supervision. Professor Olga Korostynska and Associate Professor Arvind Keprate have co-supervised Einar's master project. Professor Korostynska has done the critical review of this article.

References

- El-Rawy, M., Abd-Ellah, M. K., Fathi, H., & Ahmed, A. K. A. (2021). Forecasting effluent and performance of wastewater treatment plant using different machine learning techniques. *Journal of Water Process Engineering*, 44, 15. doi: <https://doi.org/10.1016/j.jwpe.2021.102380>
- European Commission. (2021). *Eu strategy on energy system integration*. Retrieved from https://energy.ec.europa.eu/topics/energy-system-integration/eu-strategy-energy-system-integration_en
- European Commission. (2022). *Proposal for a revised urban wastewater treatment directive*. Retrieved from https://environment.ec.europa.eu/publications/proposal-revised-urban-wastewater-treatment-directive_en
- Henze, M., Gujer, W., Mino, T., Matsuo, T., Wentzel, M. C., v.R. Marais, G., & Loosdrecht, M. C. V. (1999). Activated sludge model no.2d, asm2d. *Water Science Technology*, 39(1), 165-182.
- Ljung, L. (1999). *System identification - theory for the user* (2nd ed.). Prentice Hall. Retrieved from <https://onlinelibrary.wiley.com/doi/10.1002/047134608X.W1046>
- Ly, Q. V., Truong, V. H., Ji, B., Nguyen, X. C., Cho, K. H., Ngo, H. H., & Zhang, Z. (2022). Exploring potential machine learning application based on big data for prediction of wastewater quality from different full-scale wastewater treatment plants. *Science of the Total Environment*, 832, 12. doi: <http://dx.doi.org/10.1016/j.scitotenv.2022.154930>
- Nair, A. M., Fanta, A., Haugen, F. A., & Ratnaweera, H. (2019). Implementing and extended kalman filter for estimating nutrient composition in a sequential batch mbbf pilot plant. *Water Science Technology*, 80(2), 317-328. doi: <https://doi.org/10.2166/wst.2019.272>
- Nair, A. M., Gonzales-Silva, B. M., Haugen, F. A., Ratnaweera, H., & Østerhus, S. W. (2020). Real-time monitoring of enhanced biological phosphorus removal in a multistage ebpr-mbbf using a soft-sensor for phosphates. *Journal of Water Process Engineering*, 37(101494), 13. doi: <https://doi.org/10.1016/j.jwpe.2020.101494>
- Nermo, E. (2023). *Mpc of nutrient removal in wastewater treatment process* [Master Thesis]. Oslo Metropolitan University.
- Rudi, K., Goa, I. A., Saltnes, T., Sørensen, G., Angell, I. L., & Eikås, S. (2019). Microbial ecological processes in mbbf biofilms for biological phosphorus removal from wastewater. *Water Science Technology*, 79(8), 1467-1473. doi: <https://doi.org/10.2166/wst.2019.149>
- Tomperi, J., & Leiviskä, K. (2018). Comparison of modelling accuracy with and without exploiting automated optical monitoring information in predicting the treated wastewater quality. *Environmental Technology*, 39(11), 1442-1449. doi: <https://doi.org/10.1080/09593330.2017.1331267>